

# Birefringent filter design by use of a modified genetic algorithm

Mengtao Wen and Jianping Yao

A modified genetic algorithm is proposed for the optimization of fiber birefringent filters. The orientation angles and the element lengths are determined by the genetic algorithm to minimize the sidelobe levels of the filters. Being different from the normal genetic algorithm, the algorithm proposed reduces the problem space of the birefringent filter design to achieve faster speed and better performance. The design of 4-, 8-, and 14-section birefringent filters with an improved sidelobe suppression ratio is realized. A 4-section birefringent filter designed with the algorithm is experimentally realized. © 2006 Optical Society of America

OCIS codes: 060.2340, 230.0230.

## 1. Introduction

Fiber birefringent filters are of great interest for many applications such as dense wavelength division multiplexing, multiwavelength fiber lasers, and optical signal processing. A fiber birefringent filter consists of a certain number of birefringent optical elements between a certain number of polarizers.<sup>1-6</sup> The elements are usually of high birefringence.<sup>7,8</sup> Phase shifts are introduced between the two orthogonal components of a linearly polarized light. The polarizer is used to interfere with the two orthogonal components such that the intensity of the linearly polarized light is strengthened or weakened, depending on the shift angle between the polarizer and the polarized light.<sup>1-6,8</sup> The transmission through a birefringent filter at a given wavelength is a function of the optical retardation exhibited by each of the filter stages.<sup>1-6</sup> Adding the retardation to each stage in proper fashion makes it possible to shift the passbands and stop bands at will. Therefore, by rotating the relative angles between adjacent birefringent elements, we can obtain different spectral responses. The goal of designing a birefringent filter is to find a series of lengths and angles of the birefringent ele-

ments such that the designed spectral response best approximates the desired spectral response.<sup>3,5</sup>

Birefringent filters were first introduced to be an effective tool in astronomical research<sup>1,4,10</sup> since they are capable of transmitting monochromatic light from a broadband source. Now they have found applications in a wide variety of other disciplines such as spectroscopy, imaging, and optical telecommunication.<sup>11-15</sup> There are two types of basic birefringent filters, Lyot and Solc birefringent filters, with retardation introduced by control of the element lengths and adjacent element shift angles, respectively.<sup>1-3,5</sup>

The Lyot filter was first introduced by a French astronomer, Bernard Lyot, in 1933.<sup>1</sup> It consists of a number of alternating polarizers and birefringent plates. The length of each successive birefringent plate is twice that of the previous plate.<sup>1,16</sup> The multiple passbands are spaced by the free spectral range (FSR) of the thinnest optical element.<sup>1,16</sup> The configuration of a Lyot filter is shown in Fig. 1.

The Solc filter is another type of birefringent filter with a simpler structure than that of the Lyot birefringent filter.<sup>2,3</sup> Unlike the Lyot filter, which has one birefringent section between a pair of polarizers, the Solc filter has a number of birefringent sections between a pair of polarizers. The Solc filter can be further classified into two categories, folded and fan Solc filters. A folded Solc filter consists of alternating equal shift angles.<sup>6,17</sup> The fan Solc filter differs from the folded Solc filter in that the shift angle increases in magnitude by a constant instead of alternating in sign.<sup>17</sup>

Both Lyot and Solc filters have symmetrical structures. As pointed out by Harris *et al.*,<sup>5</sup> the shift angles

M. Wen and J. Yao (jpyao@site.uottawa.ca) are with the Microwave Photonics Research Laboratory, School of Information Technology and Engineering, University of Ottawa, Canada K1N 6N5.

Received 6 July 2005; revised 22 December 2005; accepted 30 December 2005; posted 5 January 2006 (Doc. ID 63259).

0003-6935/06/173940-11\$15.00/0

© 2006 Optical Society of America

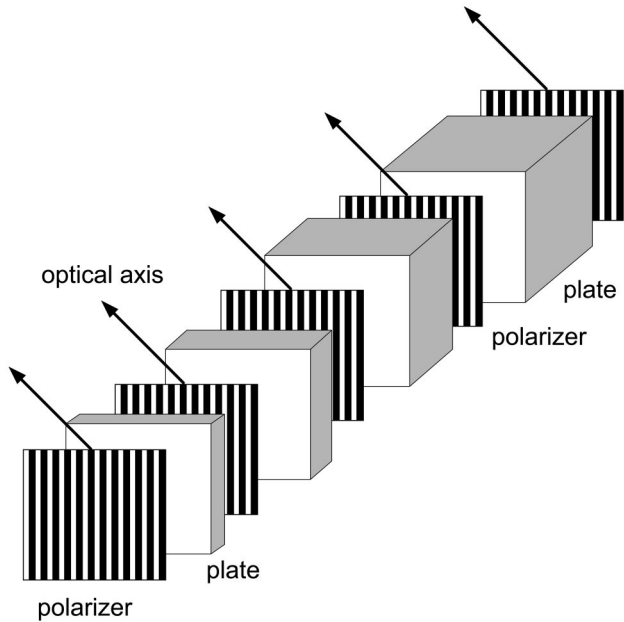


Fig. 1. Lyot filter.

between the birefringent sections can be adjusted arbitrarily to further reduce the sidelobe levels of the filter spectral responses. The Jones matrix can be used to generalize the transmission characteristic of the Solc filter with arbitrary angles.<sup>2,3,17-19</sup>

Figure 2 shows the configuration of a Solc birefringent filter with arbitrary angles. This configuration is a general form of the fan Solc filter and the folded Solc filter. As shown in the figure, the light with input  $E_{x0}$  and  $E_{y0}$  is polarized first and then travels along the  $z$  axis in a rectangular coordinate system. The face of each birefringent section is normal to the  $z$  axis. The electric field vectors of the light after the analyzer can be expressed as<sup>3</sup>

$$\begin{pmatrix} E_{A1} \\ E_{A2} \end{pmatrix} = R(\varphi_p)M(\varphi_i, \eta)P_x \begin{pmatrix} E_{x0} \\ E_{y0} \end{pmatrix}, \quad (1)$$

where  $E_{x0}$  and  $E_{y0}$  are the inputs;  $E_{A1}$  and  $E_{A2}$  are the transmitted and rejected components, respectively; and  $R(\varphi_p)$  is the matrix representing the rotation by  $\varphi_p$  and is defined as<sup>3,17</sup>

$$R(\varphi_p) = \begin{bmatrix} \cos \varphi_p & \sin \varphi_p \\ -\sin \varphi_p & \cos \varphi_p \end{bmatrix}, \quad (2)$$

where  $P_x$  denotes the input polarizer transmitting the electric vector parallel to the  $x$  axis, defined as<sup>3,17</sup>

$$P_x = \begin{bmatrix} 1 & 0 \\ 0 & 0 \end{bmatrix}, \quad (3)$$

$M(\varphi_i, \eta)$  is a matrix product of a series of rotations and retardations caused by a stack of birefringent sections; therefore<sup>3,17</sup>

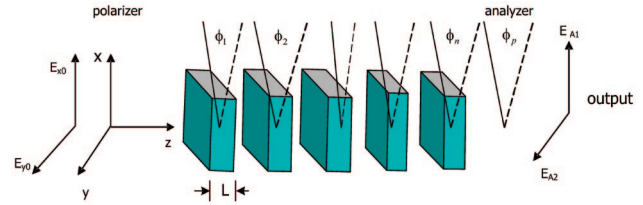


Fig. 2. (Color online) Solc filter with arbitrary angles.

$$\begin{aligned} R(\varphi_p)M(\varphi_i, \eta) &= R(\varphi_p - \varphi_n)R_\eta R(\varphi_n - \varphi_{n-1}) \\ &\quad \times R_\eta \cdots R(\varphi_2 - \varphi_1)R_\eta R(\varphi_1) \\ &= R(\theta_n)R_\eta R(\theta_{n-1})R_\eta \cdots R(\theta_1)R_\eta R(\theta_0). \end{aligned} \quad (4)$$

Here the relative rotation is<sup>3,17</sup>

$$R(\theta_i) = \begin{bmatrix} \cos \theta_i & \sin \theta_i \\ -\sin \theta_i & \cos \theta_i \end{bmatrix}. \quad (5)$$

The retardation is<sup>3,17</sup>

$$R_\eta = \begin{bmatrix} \exp(j\eta/2) & 0 \\ 0 & \exp(-j\eta/2) \end{bmatrix}, \quad (6)$$

$$\eta = 2\pi f(\Delta nL/c), \quad (7)$$

where  $\Delta n$  is the birefringence,  $L$  is the length of the birefringent section, and  $f$  is the frequency of the light.

## 2. Designing a Birefringent Filter by a Genetic Algorithm

To design a birefringent filter, one should find the shift angle and length of each birefringent section to meet the specific design requirement. Many algorithms have been proposed in the past few decades.<sup>3,5,6</sup> Harris *et al.*<sup>5</sup> assumed that the birefringent sections are equal in length and used a Fourier series approximation to calculate the filter coefficients. Chu and Town<sup>3</sup> used the Remez exchange algorithm and Pegis's method to find the polynomial, from which they used an inverse transform algorithm to find the angles. These algorithms usually require a large number of sections, by using an inverse transform to obtain a specified spectral response, since they are usually based on a particular case of birefringent filter (Solc or Lyot) and have less freedom to control the retardation of the optical elements. In this paper, we propose a modified genetic algorithm (GA) that uses the forward transform of the Jones matrix directly to find the corresponding parameters for a given birefringent filter. The birefringent filter designed by the modified GA, compared with other algorithms,<sup>3,5</sup> provides a more flexible structure and better performance in terms of the sideband suppression ratio.

In our study, we first use Solc filters as an example to describe our algorithm and assume the filter section lengths to be identical. However, the GA does not

require that the birefringent sections have identical lengths since the GA is a forward transform algorithm and can be applied to an arbitrary configuration of birefringent filters as long as the parameters (element lengths, angles) are encoded as their corresponding chromosomes. We later describe the algorithm to design another example with both the element length and the shift angles variable.

### A. Cost Function

For a low-pass filter, the desired spectral response of a filter can be expressed as  $(0, f_p, f_s, 1)$  in which  $f_p$  is the normalized pass frequency and  $f_s$  is the normalized stop frequency. The normalized desired intensity is

$$I = \left\{ \begin{array}{ll} 1 + \delta_{\text{pass}}, & 0 \leq f \leq f_p \\ \text{not of concern,} & f_p < f < f_s \\ 0 + \delta_{\text{stop}}, & f_s \leq f \end{array} \right\}, \quad (8)$$

where  $\delta_{\text{pass}}$  and  $\delta_{\text{stop}}$  are the passband and the stop band intensity deviations, respectively.

The goal of designing a Solc birefringent filter is to find a series of shift angles  $\varphi_1, \varphi_2, \dots, \varphi_n$  such that the output spectral response best approximates the desired response. The difference between the output spectral response and desired spectral response is the cost function, which is the object function that we will optimize as fitness in the GA. The cost function is represented as the least-mean-squares error. Therefore the design problem is reduced to finding the shift angles between adjacent sections such that the least-mean-squares error is minimized. The cost function can be expressed as

$$\cos t(\varphi_1, \varphi_2, \dots, \varphi_n) = \sum_{\text{passband}} |I_{\text{pass}} - 1| + W \sum_{\text{stop band}} |I_{\text{stop}}|, \quad (9)$$

where  $I_{\text{pass}}$  is the normalized passband intensity and  $I_{\text{stop}}$  is the normalized stop band intensity that comes from the Jones matrix  $R(\varphi_p)M(\varphi_i, \eta)$ .  $W$  is the weight that can be used to control the ripples of the designed spectral response; in particular, we can control those important regions such as the passband and the stop band and ignore the errors in the transition band. If we need to achieve a lower sidelobe level, then we can assign a large value of  $W$  to the stop band: for example, if we want to design a filter with  $\delta_{\text{pass}} = \pm 2$  dB and  $\delta_{\text{stop}} = -20$  dB. Since the values of  $-2$  and  $-20$  dB are about 0.6 and 0.01, respectively, if we want the passband and the stop band to have the same significance in the cost function, the weight of the stop band should be  $0.6/0.01 = 60$ . However, the large value of  $W$  assigned to the stop band might degenerate the performance of the passband and the transition band. This means that a large value of  $W$  can lead to a lower sideband level but might impair the flatness of the passband. In our design the value of  $W$  is empirically set to be between 1 and 1000,

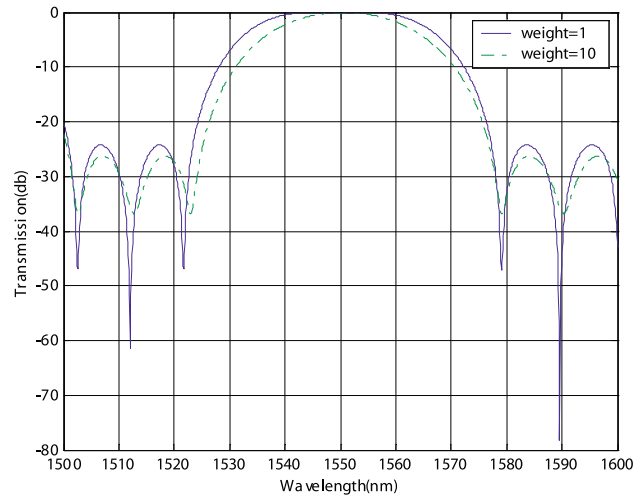


Fig. 3. (Color online) Spectral responses with different weights.

depending on the ripples allowed in the spectral responses of the passband and the stop band.

Figure 3 shows the designed spectral responses of a 4-section birefringent filter for two different weights. The dashed-dotted curve shows the Solc filter with a weight of 10 in the stop band, and the solid curve shows the Solc filter with a weight of 1 in the stop band. As shown in the figure, the Solc filter with a weight of 10 can achieve lower sidelobes; however, the passband is not as flat as the one with the weight of 1.

### B. Genetic Algorithm

The GA is an optimization algorithm that has been extensively researched in the past few years.<sup>20–23</sup> The principle of the GA is simple and direct. It imitates the process of natural evolution by maintaining a population pool.<sup>20</sup> Different individuals in nature compete for food generation after generation. The stronger individuals have a better chance of mating and will have more offspring. Their offspring inherit similar characteristics from their ancestors. Therefore the offspring of the stronger individuals might be more competent to survive than the offspring of the weaker ones. The problems that are optimized by the GA are implemented by genetic operators, including selection, crossover, and mutation.

#### 1. Encoding Scheme

Either binary encoding or floating-point (FP) encoding of the GA can be used for the optimization problems.<sup>24–26</sup> Binary encoding offers the maximum number of schemata per bit of information of any coding,<sup>20,24,25</sup> and consequently the bit-string representation of solutions has dominated genetic research. One drawback of binary encoding for real numbers is that the string length is long with high precision. The longer the length, the wider the problem space will be. Another problem with binary encoding is that the chromosome value does not correspond to the real problem space. A small difference in the chromosome may lead to a large difference

in the real parameter space, which depends on the position of the bit to be mutated. FP encoding mitigates such problems by using floating data to directly represent a real number, and the precision of the data depends on only the precision of the computer. Our study demonstrates that for the birefringent filter design, FP encoding performs more consistently than binary encoding.

FP encoding gives the chromosomes more adaptability. The shift angle  $\varphi_i$  can be encoded as

$$\varphi_i = \pi(r - 0.5), \quad (10)$$

where  $r$  is a random variable ranging from 0 to 1 and  $\varphi_i$  is the shift angle ranging from  $-\pi/2$  to  $\pi/2$ .

## 2. Genetic Operators

The selection operator used in this paper is the tournament selection scheme<sup>27</sup> based on the fitness rank in a population pool.

The arithmetical crossover<sup>20</sup> is used to generate new offspring. If two chromosomes  $\varphi^v = (\varphi_1^v, \varphi_2^v, \dots, \varphi_n^v)$  and  $\varphi^w = (\varphi_1^w, \varphi_2^w, \dots, \varphi_n^w)$  are to be crossed in the position  $k$ , the resulting offspring are  $(\varphi_1^v, \varphi_2^v, \dots, \varphi_k^{v+}, \dots, \varphi_n^v)$  and  $(\varphi_1^w, \varphi_2^w, \dots, \varphi_k^{w+}, \dots, \varphi_n^w)$ , that is,

$$\begin{aligned} \varphi_k^{v+} &= (1 - \alpha)\varphi_k^v + \alpha\varphi_k^w, \\ \varphi_k^{w+} &= (1 - \alpha)\varphi_k^w + \alpha\varphi_k^v, \end{aligned} \quad (11)$$

where  $\alpha$  is a dynamic parameter calculated in a given context of  $\varphi_k^v$ ,  $\varphi_k^w$  and their range determines how close the offspring are to their parents.

Since we use FP encoding, the mutation of each gene  $\varphi_k^t$  can be expressed directly as

$$\varphi_k^{t+1} = \varphi_k^t \pm \Delta, \quad (12)$$

where  $\varphi_k^v$  is the  $k$ th gene of the  $t$ th generation and  $\Delta$  is the step size that determines how a gene is mutated. The step size  $\Delta$  is an important function for controlling the convergence speed of the genetic process.<sup>20,21</sup> The step size  $\Delta$  should be a large value in the beginning to enable the genetic process to search a wider area and decrease gradually to avoid the genetic drift. The step size can be expressed as

$$\Delta = \pi r \left[ 1 - \left( \frac{t}{T} \right)^x \right], \quad (13)$$

where  $r$  is a random variable ranging from 0 to 1,  $t$  is the number of the current iteration,  $T$  is the total number of iterations, and  $x$  is a variable that determines the convergence speed of the step size that ranges from 0 to 1.

In our design, the population size, mutation probability, and crossover probability are common values as used in other GAs.<sup>20–23</sup> The elitism principle is used to increase the selection pressure and to avoid the dete-

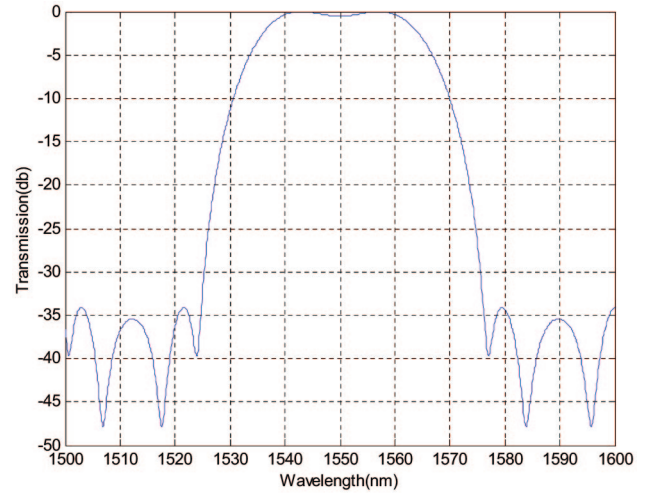


Fig. 4. (Color online) Spectral response of an 8-section birefringent filter.

rioration of the best individual by other genetic operators such as mutation. To avoid the premature convergence, what we usually can do is increase the mutation probability. Another parameter  $x$  in Eq. (13) can also be used to control the convergence speed and to avoid the premature convergence. A larger value of  $x$  can lead to a lower convergence speed. For a large-section birefringent filter design, we usually use a relatively large value of  $x$  to reduce the convergence speed.

## 3. Designing Examples by the Normal Genetic Algorithm

Before we start the design, several parameters need to be specified first. As shown in Eq. (7),  $\eta = 2\pi f(\Delta nL/c)$ . That means the phase shift  $\eta$  is determined by the birefringence  $\Delta n$  and the section length  $L$ . To determine the center wavelength, the phase shift  $\eta$  should be  $2k\pi$  ( $k$  is an integer) to have the maximum output. Therefore,

$$\begin{aligned} \eta &= 2\pi f(\Delta nL/c) = 2\pi(\Delta nL/\lambda) = 2k\pi, \\ k\lambda &= \Delta nL. \end{aligned} \quad (14)$$

Equations (14) mean that  $\Delta nL$  must be an integer times the center wavelength. If the birefringence of the fiber is  $4 \times 10^{-4}$  and the center wavelength is 1550 nm, the element length can be 7.75 cm, 15.5 cm, etc. The FSR can be calculated as<sup>3</sup>

$$\text{FSR} = \frac{c}{\Delta nL}. \quad (15)$$

Therefore, if the section length is 7.75 cm, the FSR is  $9.667 \times 10^{12}$  Hz.

For our design, we specify the required spectral response to be (0, 0.2, 0.5, 1), in which the pass frequency  $f_{\text{pass}} = 0.2$  and the stop frequency  $f_{\text{stop}} = 0.5$ . The requirement for the passband is  $I_{\text{pass}} \pm \delta \leq 0 \pm 2$  db.

Figure 4 shows the spectral response of an 8-section birefringent filter designed by the normal GA. From the figure we can find that its sidelobe suppression is about 33 dB.

#### 4. Designing a Birefringent Filter by a Modified Genetic Algorithm

##### A. Reducing Problem Space

The performance of the GA is affected to some extent by the problem space. The larger the problem space, the poorer the performance might be.<sup>20</sup> To achieve a comparative performance for the design with a large problem space, one of the methods is to enlarge the population size such that the GA has more candidates to search in wider areas.<sup>20</sup> However, a large population size will increase the computation time. In practice, we have to make a compromise between the computation speed and the performance.

Another method for improving the performance is to reduce the problem space directly since the shift angle is within  $(-\pi/2, \pi/2)$  and the size of the problem space depends on the precision. Our method is to perform the search hierarchically. We called the first run a rough search. The purpose of the rough search is to locate the individual quickly in a certain range of the problem space. If we set the mutation step size to be integer times of  $\Delta\varphi$  and the shift angle found by the GA is  $\varphi_i$ , then the final angle should be located in the range of  $[-\Delta\varphi + \varphi_i, \Delta\varphi + \varphi_i]$ . The dimensions of  $\Delta\varphi$  will determine the size of the problem space. If  $\Delta\varphi$  is large, the GA will work more consistently; however, a large  $\Delta\varphi$  might cover many local optima and will affect the search by the second run. Therefore there is a compromise in choosing  $\Delta\varphi$ . In our design,  $\Delta\varphi$  is empirically set to be  $0.5^\circ$ .

The second run is called the precise search, and we use the simulated annealing (SA) algorithm, another random optimization algorithm,<sup>28,29</sup> to replace the GA to accurately locate the individual. The SA algorithm, introduced by Kirkpatrick and co-workers in 1983, was proposed based on an analogy with the annealing of solids: The object function to be minimized is analogous to the energy of solids, and the control parameter is analogous to the temperature of solids.<sup>28,29</sup> One advantage of SA over the GA is that it can precisely locate the optimum in a narrow area faster than the GA since the operator of the SA algorithm is simply mutation, whereas the operator of the GA is complicated, and those operations might cause the GA to deviate from the precise position. Although our algorithm has multiple runs, since the algorithm converges much faster in a smaller problem space, the total time consumed is reduced. Since in the second run the GA has already found the nearly optimum solution, the cooling temperature for SA must be high to avoid drift from that area.

##### B. Family Solutions and Processed Fitness

As our study shows, the solution to a given birefringent filter is not unique. Different combinations of shift angles can be applied to realize the same spec-

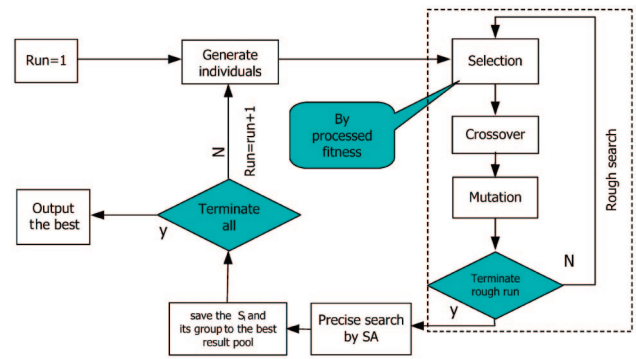


Fig. 5. (Color online) Flow chart of the modified GA.

ified spectral response with similar performances. Although the GA has a large population size and can be used to produce family solutions, its individuals usually converge to an identical individual finally. Therefore, in practice we usually obtain only one solution for each run. One way to obtain family solutions is to run the algorithm many times. Since the GA starts the search from random individuals, it might reach different outcomes with different runs.

The search for family solutions by different runs of the GA may also produce the same results by different runs since the GA does not know what it has explored in the previous search and may fall into the same area. Consequently a simple repeat is ineffective and time consuming. One way to solve this problem is to make the GA memorize what it has done and not explore those already explored areas. After the GA records those optimal shift angles that it has discovered, when the successive runs approach that area, then the algorithm can force it to leave that area.

The processed fitness<sup>30,31</sup> can be used to memorize the area already explored by the GA. Suppose that we have two series of angles  $(\alpha_1, \alpha_2, \dots, \alpha_n)$  and  $(\beta_1, \beta_2, \dots, \beta_n)$ , where  $(\alpha_1, \alpha_2, \dots, \alpha_n)$  is the solution already found. The Euclidean distance can be used to measure the distance between  $(\alpha_1, \alpha_2, \dots, \alpha_n)$  and  $(\beta_1, \beta_2, \dots, \beta_n)$ .<sup>30</sup> If the distance between them is smaller than a certain value (section radius), we may consider that  $(\beta_1, \beta_2, \dots, \beta_n)$  is now exploring the already explored area of  $(\alpha_1, \alpha_2, \dots, \alpha_n)$ , and we can force  $(\beta_1, \beta_2, \dots, \beta_n)$  to leave this area.

Forcing an individual to leave an area can be implemented by reducing the opportunities the individual has to survive when it is close to that area. It is implemented by lowering the fitness in accordance with the distance to the best individual in that area. Therefore the new fitness of an individual  $x$  can be expressed as<sup>30,31</sup>

$$F'(x) = F(x)G(x, s_1, s_2, \dots, s_n), \quad (16)$$

where  $F'(x)$  is the new fitness, which is also called the processed fitness.  $F(x)$  is the original fitness and  $G(x, s_1, s_2, \dots, s_n)$  is an evaluation function that corresponds to the distance between the individual  $x$  and those already-found best individuals

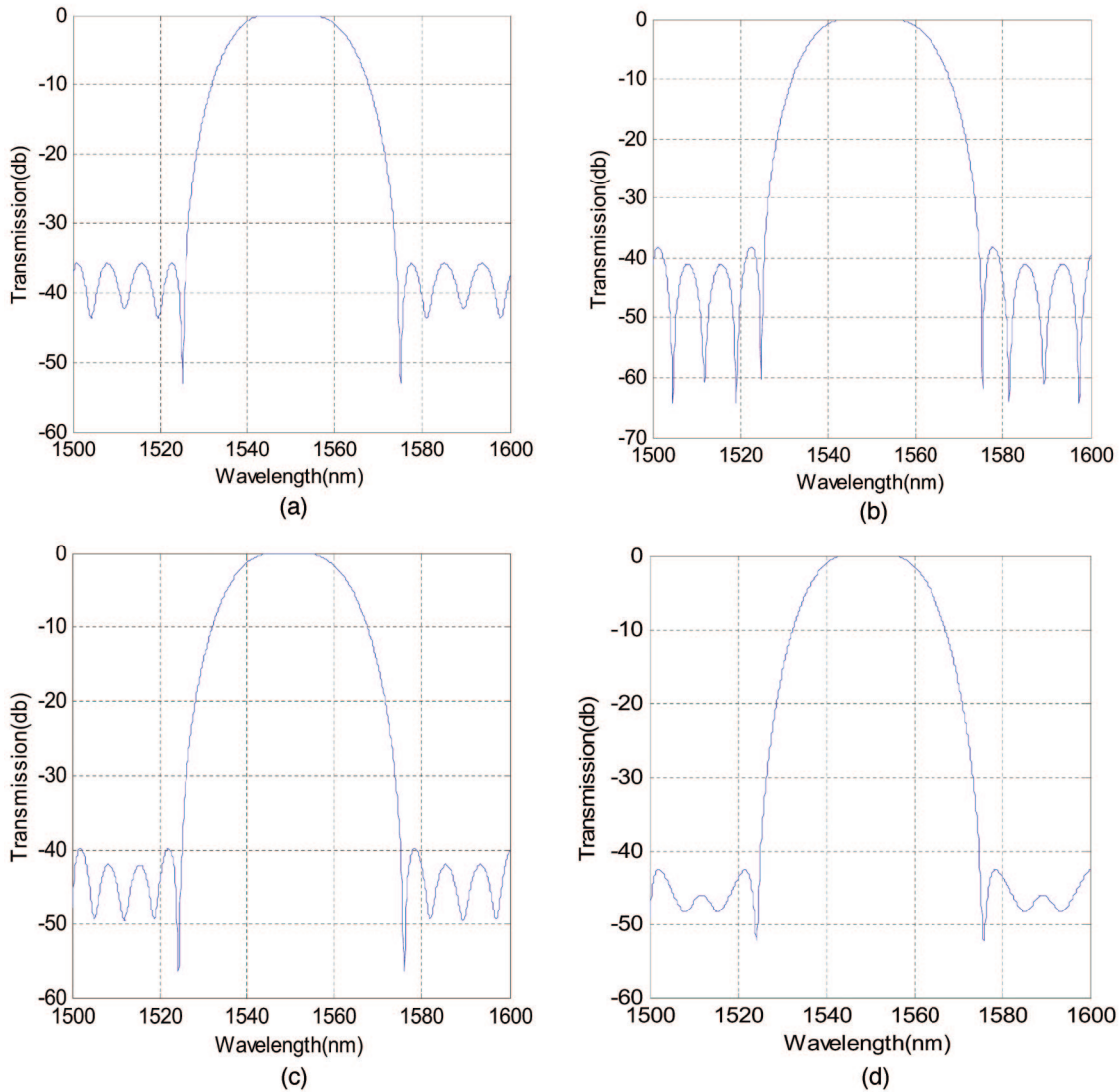


Fig. 6. (Color online) Family of an 8-section birefringent filter designed by the modified GA.

$(s_1, s_2, \dots, s_n)$ .<sup>30,31</sup> The closer the distance, the smaller the  $G(x, s_1, s_2, \dots, s_n)$  will be. The evaluation function used in our design is given as<sup>30</sup>

$$G(x, s_1, s_2, \dots, s_n) = \begin{cases} [d(x, s_1, s_2, \dots, s_n)/r]^\alpha, & d(x, s_1, s_2, \dots, s_n) < r \\ 1, & \text{otherwise} \end{cases}, \quad (17)$$

where  $d(x, s_1, s_2, \dots, s_n)$  is the minimum Euclidean distance of the individual  $x$  and those already-found best individuals  $(s_1, s_2, \dots, s_n)$ ,  $\alpha$  is a parameter (it is 5 in our example), and  $r$  is the section radius that is in direct proportion to the number of birefringent sections and inverse to the number of solutions.<sup>30</sup>

As a random search algorithm, the GA cannot avoid falling into a local optimum completely. Therefore, to let the GA know what it has done so it will not

repeat exploring the already explored area is helpful for the improvement of the GA. Furthermore, the GA will discover a serial of solutions by different runs.

Some of these solutions are only local optima, and in practice we can set a certain standard such as the sidelobe level to eliminate those local optima.

### C. Reducing Search Space by Creating Group Solutions

The search space can be further reduced in the birefringent filter design. For an  $n$ -section ( $n$  is an even integer) birefringent filter, the shift angle  $(\theta_0, \theta_1, \theta_2, \dots, \theta_n)$  represents a certain spectral response. We

**Table 1. Comparison of Cost Functions between the Normal Genetic Algorithm and the Modified Genetic Algorithm**

| Method   | Maximum Cost Function | Minimum Cost Function | Average Cost Function |
|--|-----------------------|-----------------------|-----------------------|
| Normal GA  | 7.3892                | 1.7634                | 4.3856                |
| Use hierarchical search only                                     | 7.0292                | 1.0825                | 3.6009                |
| Use processed fitness only                                       | 8.8773                | 1.1408                | 4.1445                |
| Modified GA (use both hierarchical search and processed fitness) | 8.2798                | 1                     | 3.5027                |

can prove that for  $(\theta_0, \theta_1, \theta_2, \dots, \theta_n)$ , every two angles that are symmetrical to the center angle  $\theta_{n/2}$  can be exchanged without altering the output spectral response. We briefly describe the derivation of this theory in two steps.

Step 1: For a 2-section filter, the output is

$$R(\theta_2)R_\eta R(\theta_1)R_\eta R(\theta_0) = \begin{bmatrix} \cos \theta_2 & \sin \theta_2 \\ -\sin \theta_2 & \cos \theta_2 \end{bmatrix} \begin{bmatrix} \exp(j\eta/2) & 0 \\ 0 & \exp(-j\eta/2) \end{bmatrix} \times \begin{bmatrix} \cos \theta_1 & \sin \theta_1 \\ -\sin \theta_1 & \cos \theta_1 \end{bmatrix} \begin{bmatrix} \exp(j\eta/2) & 0 \\ 0 & \exp(-j\eta/2) \end{bmatrix} \times \begin{bmatrix} \cos \theta_0 & \sin \theta_0 \\ -\sin \theta_0 & \cos \theta_0 \end{bmatrix}. \quad (18)$$

Let

$$\begin{bmatrix} \exp(j\eta/2) & 0 \\ 0 & \exp(-j\eta/2) \end{bmatrix} \begin{bmatrix} \cos \theta_1 & \sin \theta_1 \\ -\sin \theta_1 & \cos \theta_1 \end{bmatrix} \times \begin{bmatrix} \exp(j\eta/2) & 0 \\ 0 & \exp(-j\eta/2) \end{bmatrix} = \begin{bmatrix} A & -B^* \\ B & A^* \end{bmatrix}, \quad (19)$$

where  $A = \exp(j\eta)\cos \theta_1$  and  $B = -\sin \theta_1$ , then the intensity can be expressed as

$$|A \cos \theta_2 \cos \theta_0 - A^* \sin \theta_2 \sin \theta_0 + B \sin \theta_2 \cos \theta_0 + B^* \cos \theta_2 \sin \theta_0|^2;$$

therefore the intensity must be the same if the  $\theta_2$  and  $\theta_0$  are exchanged.

Step 2: Use the induction method. If the  $n$ -section birefringent filter agrees with this theory, then for an  $(n + 2)$ -section filter, since the output of the  $n$ -section filter can also be expressed as

$$\begin{bmatrix} A & -B^* \\ B & A^* \end{bmatrix},$$

the intensity can be expressed as

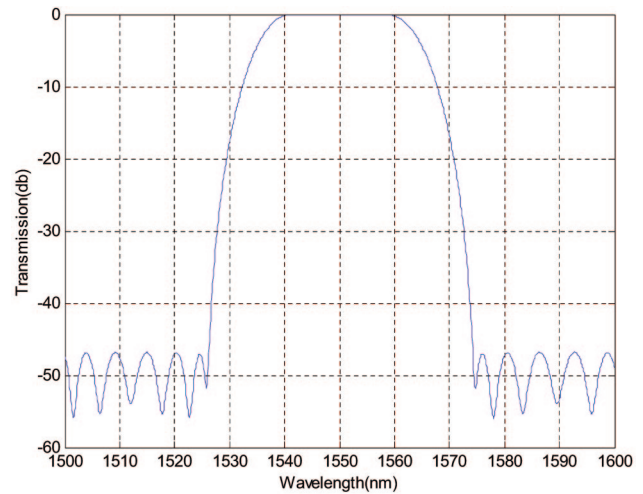


Fig. 7. (Color online) 14-section birefringent filter designed by the modified GA.

$$|A \cos \theta_{n+2} \cos \theta_0 - A^* \sin \theta_{n+2} \sin \theta_0 + B \sin \theta_{n+2} \cos \theta_0 + B^* \cos \theta_{n+2} \sin \theta_0|^2,$$

which also satisfies the theory.

This theory tells us that, for each solution  $(\theta_0, \theta_1, \theta_2, \dots, \theta_n)$ , we will have  $2^{n/2}$  solutions that can realize the same spectral response. Therefore, for every solution we find, we can use the processed fitness to disable the search for the other  $2^{n/2}$  areas.

#### D. Flow Chart of Our Algorithm

By summarizing all the steps discussed above, we have the flow chart of the algorithm, shown in Fig. 5.

#### E. Designing Examples by the Modified Genetic Algorithm

We use the modified GA discussed above to redesign the 8-section birefringent filter. The corresponding spectral responses are shown in Fig. 6.

As shown in Fig. 6, the modified GA provides a series of solutions to the required spectral response. The spectral response shown in Fig. 6(a) has a similar sideband suppression ratio as that in Fig. 4 achieved by use of a normal GA, but their design angles are totally different. Figures 6(b), 6(c), and 6(d) have a higher sideband suppression ratio than the design by the normal GA, and at the same time the flatness is within our requirements. Figure 6(d) achieves a sideband suppression ratio of better than 42 dB. Therefore, as far as both the passband and the stop band are concerned, the design shown in Fig. 6(d) has the best performance. The results also indicate that the modified GA not only improves the performance but also provides different outputs that we can choose as our desired solution.

To further analyze the three methods, the hierarchical search, the processed fitness, and the use of the symmetrical principle of the birefringent filter to reduce the problem space on the performance of the GA, we use an 8-section birefringent filter to test these methods separately. Since the symmetrical principle

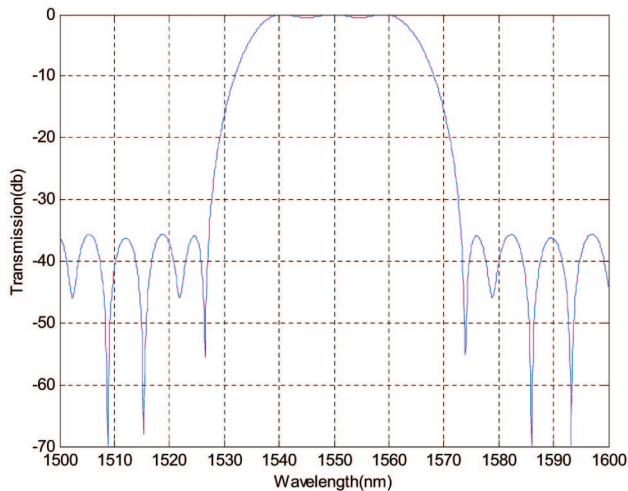


Fig. 8. (Color online) 4-section birefringent filter with nonidentical section lengths.

of the birefringent filter is implemented by reducing the processed fitness, it can be classified into the second method. Each test runs 100 times, and the results are summarized in Table 1.

The cost functions are normalized based on the minimum cost function of the modified GA. From the table we can find that the hierarchical search improves the performance more than the processed fitness since the average cost function by the hierarchical search is 3.6009, whereas that by the processed fitness is 4.1445. In locating the best individuals, the hierarchical search also performs better. Although the processed fitness acquires a worse individual than the normal GA (the maximum cost function of it is larger), the best individual it acquires is much better than that of the normal GA. This is because the processed fitness memorized those already-explored spaces and hence will not be trapped in the local optimum as easily as the normal GA. From our tests, we also found that the modified GA reduces the overall computation time by 9% compared with the normal GA. Although the methods we discussed above increase the algorithm complexity for each iteration, these methods reduce the problem space for the GA; hence the overall iterations are reduced and the total computation time is reduced too.

### 5. Comparison of the Modified Genetic Algorithm with Other Algorithms

The design of a birefringent filter by a random search algorithm has been reported in recent years.<sup>6,32</sup> These algorithms explored the field of filter designs that used to be governed by the conventional digital filter design algorithms.<sup>3,5</sup> However, as their results show in Refs. 6 and 32, the performance still cannot reach those designed by the conventional digital filter design algorithms, as far as the sidelobe level is concerned. Chu and Town<sup>3</sup> proposed using a digital filter algorithm to determine an optimal polynomial approximation to obtain a specified finite impulse re-

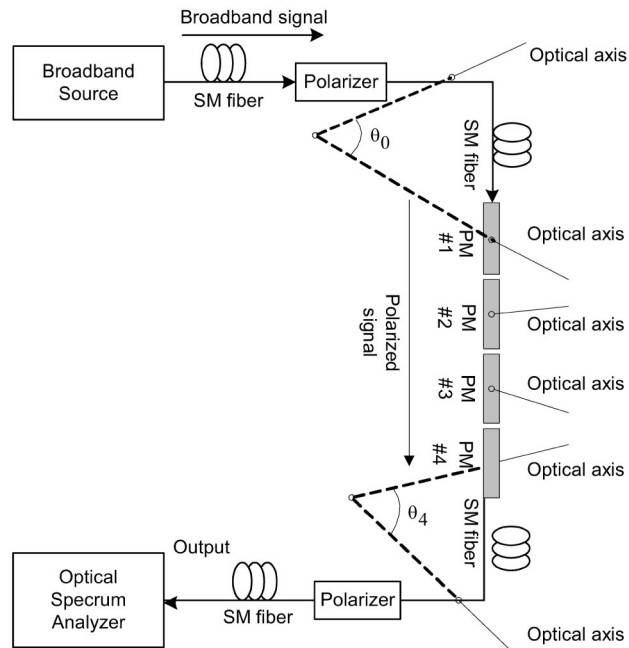


Fig. 9. Experimental setup. SM, single-mode; PM, polarization-maintaining fiber.

sponse. In their example, they used a 14-section birefringent filter to design a bandpass filter with a desired spectral response (0, 0.2, 0.5, 1) and they achieved a sideband suppression ratio of about 42 dB. To compare the performance, we use the modified GA to design a 14-section birefringent filter with all the other parameters identical to those in Ref. 3. The designed shift angles from section number 0 to 14 are  $-1.1295, -0.8743, 0.2239, -1.1757, -0.5691, 0.7228, 0.4879, -1.3058, 0.3929, 0.0682, 0.4697, 1.1741, -0.4386, 0.5856, \text{ and } 1.3265$ .

As Fig. 7 shows, the birefringent filter designed by the modified GA has a sideband suppression level of about 47 dB. The passband flatness of the filter by the modified GA is also better than that in the example of Ref. 3, and the deviation of the passband is within 0.3 dB, whereas the deviation of the passband of the example in Ref. 3 is 1 dB. Compared with the example in Ref. 3, the modified GA improves the sideband level by about 5 dB and the passband flatness by about 0.7 dB. Furthermore, the 8-section filter shown in Fig. 6(d) has a sideband suppression ratio of 42 dB, which is identical to that of a 14-section filter in Ref. 3. This indicates that filters designed by the modified GA can reach the same sideband suppression ratio with fewer filter sections.

Therefore we can say that the modified GA outperformed the conventional digital filter design algorithm at least in some cases. There are two more advantages of the GA over the conventional digital filter design algorithm: The first, as we described above, is that the GA can obtain family solutions easily. The second is that the GA can design the birefringent filter with more flexible structures. The Lyot filter and Solc filter are two special examples of birefringent filters. Our designs presented above are Solc birefringent filters with identical section lengths

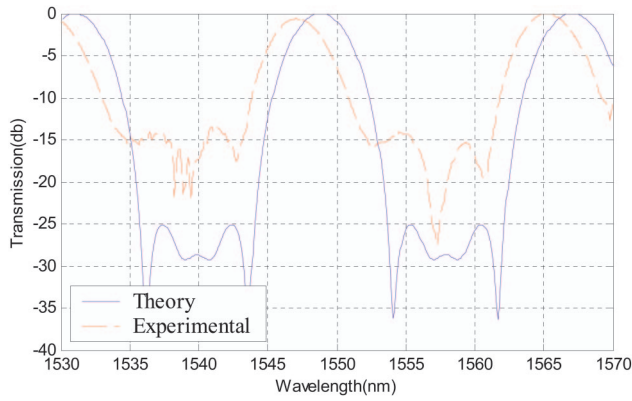


Fig. 10. (Color online) Theoretical (solid curve) and experimental (dashed curve) spectral responses.

and arbitrary angles. A more general birefringent filter is the one for which both the section lengths and the shift angles are adjustable. The design for the filter with both variable lengths and angles is summarized as below:

1. For an  $n$ -section birefringent filter, the chromosome is represented as  $(\varphi_1, \varphi_2, \dots, \varphi_{n+1}, l_1, l_2, \dots, l_n)$ ; here  $\varphi_i$  is the shift angle between the  $(i-1)$ th element and the  $i$ th element,  $l_i$  is the length of the  $i$ th element;  $l_i$  is an integer times the shortest element length, which is determined by Eqs. (14).
2. The genetic operators are categorized into two groups: the group of shift angles and the group of lengths. They are characterized by different step sizes and different ranges.
3. The calculation of the section radius is modified to adapt to the group range. An individual is considered to be in the same section only when its fiber element length is the same as the individual in that area.

Figure 8 shows the output spectral response of a 4-section birefringent filter with nonidentical section lengths. The result achieves a performance similar to that of the 8-section filter when the normal GA is used. The simulation results demonstrate that birefringent filters with adjustable lengths and angles can produce a better output than those with only adjustable angles. The filters with both adjustable lengths and angles can be viewed as a special type of birefringent filter. The fiber elements with the length integer times as long as the shortest element can be viewed as formed by several of the shortest elements and the shift angles between these shortest elements are 0. Therefore the improvement of performance is actually realized by the increase of section numbers.

## 6. Experiments

### A. Experiment Setup

From the theoretical model and the simulation, a 4-section identical-length birefringent filter is fabricated and tested. The reason that we use fewer sec-

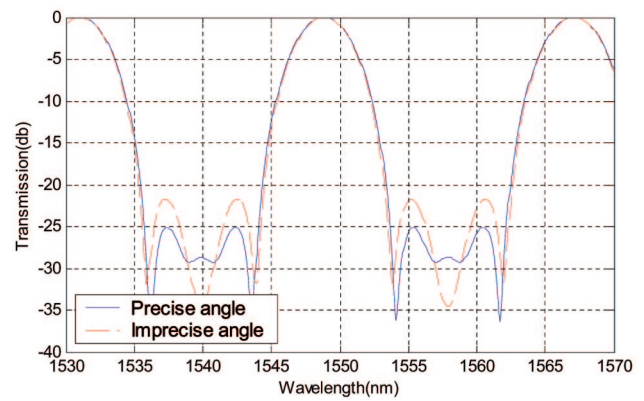


Fig. 11. (Color online) Precise angles (solid curve) versus angles with up to  $1^\circ$  error (dashed curve).

tions is the fabrication difficulty. The experimental setup is shown in Fig. 9.

The filter consists of 4-section polarization-maintaining (PM) fibers that are spliced by a PM splicer with the shift angles designed by the GA. Each end of the PM fiber is spliced to a single-mode fiber that is connected to a fiber polarizer. The fiber polarizers are used to control the input and output shift angles of the birefringent filter. In addition, the input polarizer converts the unpolarized light from the broadband source to linearly polarized light. The spectral response is observed on an optical spectrum analyzer.

The angular resolutions of the polarizers and the splicer that we use for our experiments are  $1^\circ$ ; therefore we have to round off the design results to integer numbers. The parameters of the PM fiber that we used in our experiments are as follows: birefringence;  $4 \times 10^{-4}$ ; section length, 33.3 cm. The FSR calculated based on Eq. (15) is  $2.292 \times 10^{12}$  Hz.

### B. Experiment Results and Discussions

To do the experiment with a splicer resolution of  $1^\circ$ , we have to round off the angles to integers. The rounding of the angles will affect the output spectrum. Based on our simulation, the extent of the influence on the stop band suppression ratio usually ranges from 1 to 3 dB.

The theoretical and experimental spectral responses are shown in Fig. 10. From the figure we can find that the period of the experimental spectral response agrees well with that of the theoretical response. The shapes of the experimental and theoretical responses are also close. However, the theoretical sideband suppression ratio is 25 dB, whereas the sideband suppression ratio obtained experimentally is only 14 dB, about 11 dB less than the theoretical result. Furthermore, the center wavelength is drifting a little away from the theoretical center wavelength.

To find the reasons that lead to these discrepancies, we intentionally introduce some errors into the shift angles and the birefringent section lengths. The re-

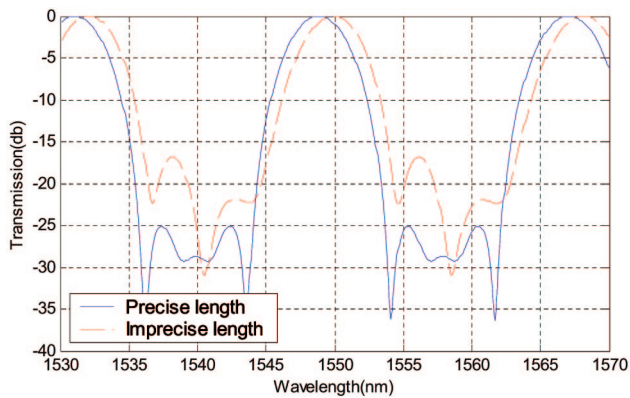


Fig. 12. (Color online) Precise lengths (solid curve) versus imprecise lengths up to 1 mm error (dashed curve).

sponses with shift angle errors and fiber length errors are shown in Figs. 11 and 12, respectively.

From Fig. 11 we find that the angle errors will influence the sideband suppression ratio, but the center wavelength is not affected. From Fig. 12 we find that the length errors have a great effect on the output spectral response. It will affect not only the sideband suppression ratio but also the center wavelength. From Eq. (13), we know that the section length is inversely proportional to the fiber birefringence. To reduce the influence of length errors on the center wavelength, a PM fiber with a smaller birefringence may be used. Another solution to this problem is to use integrated optical waveguides. Since the waveguide length can be controlled precisely, the spectral response of the birefringent-filter-based optical waveguides can provide precise spectral response.

## 7. Conclusions

A modified GA has been proposed for designing birefringent filters. The modified GA uses two hierarchical searches to reduce the problem space and to use the processed fitness to memorize those already-explored areas, to get multiple outputs, and to improve the performance. The simulation results showed that the modified GA can search in a wider range and get lower sidelobe levels compared with the normal GA. When it is compared with the conventional digital filter design algorithm, the proposed algorithm can provide a lower sidelobe level. In addition, the filter design using the proposed algorithm can design filters with more flexible structure. The birefringent filter was fabricated and experimentally verified. The implementation errors were also investigated. The study showed that the errors in section lengths would not only affect the center wavelength but also the sidelobe suppression ratio, whereas the errors in the shift angles would affect the sidelobe errors.

## References

1. J. W. Evans, "The birefringent filter," *J. Opt. Soc. Am.* **39**, 229–242 (1949).

2. J. W. Evans, "Solc birefringent filter," *J. Opt. Soc. Am.* **48**, 142–146 (1958).
3. R. H. Chu and G. Town, "Birefringent filter synthesis by use of a digital filter design algorithm," *Appl. Opt.* **41**, 3412–3418 (2002).
4. F. K. von Willisen, "A tunable birefringent filter," *Appl. Opt.* **5**, 97–104 (1966).
5. S. E. Harris, E. O. Ammann, and I. C. Chang, "Optical network synthesis using birefringent crystals. I. Synthesis of lossless networks of equal-length crystals," *J. Opt. Soc. Am.* **54**, 1267–1279 (1964).
6. Z. Zalevsky, D. Mendlovic, and E. Marom, "Tunable birefringent filters—optimal iterative design," *Opt. Express* **10**, 1534–1541 (2002).
7. A. J. Kemp, G. J. Friel, T. K. Lake, R. S. Conroy, and B. D. Sinclair, "Polarization effects, birefringent filtering, and single-frequency operation in lasers containing a birefringent gain crystal," *IEEE J. Quantum Electron.* **35**, 228–235 (2000).
8. B. M. Schiffman and L. Young, "Birefringent filter for millimeter waves," *IEEE Trans. Microwave Theory Tech.* **16**, 351–360 (1968).
9. J. M. Becker, "High-resolution measurements of photosphere and sun-spot velocity and magnetic fields using a narrow-band birefringent filter," *Sol. Phys.* **3**, 258–263 (1968).
10. J. M. Beckers, L. Dickson, and R. S. Joyce, "Observing the sun with a fully tunable Lyot–Ohman filter," *Appl. Opt.* **14**, 2061–2066 (1975).
11. D. Bonaccini and F. Stauffer, "High resolution solar bidimensional spectroscopy with a universal birefringent filter in tandem with a Fabry–Perot interferometer—Tests and experimental results," *Astron. Astrophys.* **229**, 272–278 (1990).
12. T. Kimura, M. Saruwatari, and K. Otsuka, "Birefringent branching filters for wideband optical FDM communications," *Appl. Opt.* **12**, 373–379 (1973).
13. Y. Fujii and J. Minowa, "Four-channel wavelength multiplexing composed of phase plates and polarizing beam splitters," *Appl. Opt.* **28**, 1305–1308 (1989).
14. A. Carballar, M. A. Muriel, and J. Azafi, "Fiber grating filter for WDM systems: an improved design," *IEEE Photon. Technol. Lett.* **11**, 694–696 (1999).
15. P. Yeh, W. Gunning, R. Hall, and J. Tracy, "Dispersive birefringent filters for laser communications," *IEEE J. Quantum Electron.* **17**, 2424 (1981).
16. L. J. November and F. Stauffer, "Derivation of the universal wavelength tuning formula for a Lyot birefringent filter," *Appl. Opt.* **23**, 2333–2341 (1984).
17. Y. Zhou, L. R. Liu, J. Zhang, D. Liu, and Z. Luan, "Nearly-off-axis transmissivity of Solc birefringent filters," *J. Opt. Soc. Am. A* **20**, 733–740 (2003).
18. A. Lien, "A detailed derivation of extended Jones matrix representation for twisted nematic liquid crystal displays," *Liq. Cryst.* **22**, 171–175 (1997).
19. S. Y. Lu and R. A. Chipman, "Homogeneous and inhomogeneous Jones matrices," *J. Opt. Soc. Am. A* **11**, 766–774 (1994).
20. Z. Michalewicz, *Genetic Algorithms + Data Structures = Evolution Programs*, 2nd ed. (Springer-Verlag, 1994).
21. A. E. Eiben, R. Hinterding, and Z. Michalewicz, "Parameter control in evolutionary algorithms," *IEEE Trans. Evol. Comput.* **3**, 124–141 (1999).
22. J. A. Vasconcelos, J. A. Ramirez, R. H. C. Takahashi, and R. R. Saldanha, "Improvements in genetic algorithms," *IEEE Trans. Magn.* **37**, 3414–3417 (2001).
23. R. L. Haupt and S. E. Haupt, *Practical Genetic Algorithms* (Wiley, 1998).
24. J. R. Perez and J. Basterrechea, "Near to far-field transformation using GA based optimization: real versus binary encoding

- schemes," in *Antennas and Propagation Society International Symposium* (IEEE, 2004), pp. 1122–1125.
25. S. Rochet, M. Slimane, and G. Venturini, "Epistasis for real encoding in genetic algorithms," in *Proceedings of the Australian and New Zealand Conference on Intelligent Information Systems* (IEEE, 1996), pp. 268–271.
  26. V. S. Gordon and T. J. Slocum, "The knight's tour—Evolutionary vs. depth-first search," in *Congress on Evolutionary Computation* (IEEE, 2004), pp. 1435–1440.
  27. K. Sastry and D. E. Goldberg, "Modeling tournament selection with replacement using apparent added noise," in *Intelligent Engineering Systems through Artificial Neural Networks* (American Society of Mechanical Engineering, 2001), pp. 129–134.
  28. S. Kirkpatrick, C. D. Gelatt, and M. P. Vecchi, "Optimization by simulated annealing," *Science* **220**, 671–680 (1983).
  29. S. Kirkpatrick, "Optimization by simulated annealing: quantitative studies," *J. Stat. Phys.* **34**, 975–986 (1984).
  30. D. Beasley, D. R. Bull, and R. R. Martin, "A sequential niche technique for multimodal function optimization," *Evol. Comput.* **1**, 101–125 (1993).
  31. H. Sakanashi and Y. Kakazu, "Co-evolving genetic algorithm with filtered evaluation function," in *IEEE Symposium on Emerging Technologies and Factory Automation* (IEEE, 1994), pp. 454–457.
  32. J. Xiong, F. Yu, and Y. He, "Direct design of a polarization interference filter by genetic algorithm," *Opt. Eng.* **43**, 1200–1205 (2004).